Pharmaceutical Research, Vol. 23, No. 4, April 2006 (© 2006)
DOI: 10.1007/s11095-006-9780-0

Research Paper

Pharmacokinetic Consequences of Active Drug Efflux at the Blood–Brain Barrier

Stina Syvänen,[1,2] Rujia Xie,[1,3] Selma Sahin,[1,4] and Margareta Hammarlund-Udenaes[1,5]

Received September 2, 2005; accepted December 16, 2005

Purpose. The objective of this simulation study was to investigate how the nature, location, and capacity of the efflux processes in relation to the permeability properties influence brain concentrations.
Methods. Reduced brain concentrations can be due to either influx hindrance, a gatekeeper function in the luminal membrane, which has been suggested for ABCB1 (P-glycoprotein), or efflux enhancement by transporters that pick up molecules on one side of the luminal or abluminal membrane and release them on the other side. Pharmacokinetic models including passive transport, influx hindrance, and efflux enhancement were built using the computer program MATLAB. The simulations were based on experimentally obtained parameters for morphine, morphine-3-glucuronide, morphine-6-glucuronide, and gabapentin.
Results. The influx hindrance process is the more effective for keeping brain concentrations low. Efflux enhancement decreases the half-life of the drug in the brain, whereas with influx hindrance the half-life is similar to that seen with passive transport. The relationship between the influx and efflux of the drug across the blood–brain barrier determines the steady-state ratio of brain to plasma concentrations of unbound drug, $K_{p,uu}$.
Conclusions. Both poorly and highly permeable drugs can reach the same steady-state ratio, although the time to reach steady state will differ. The volume of distribution of unbound drug in the brain does not influence $K_{p,uu}$, but does influence the total brain-to-blood ratio K_p and the time to reach steady state in the brain.

KEY WORDS: ABCB1 (P-glycoprotein); active efflux transport; blood–brain barrier; gabapentin; OAT3; opioids; permeability; pharmacokinetics.

[1] Division of Pharmacokinetics and Drug Therapy, Department of Pharmaceutical Biosciences, Uppsala University, Box 591, 751 24 Uppsala, Sweden
[2] Uppsala Imanet, Box 967, 751 09 Uppsala, Sweden
[3] Pfizer Inc, Sandwich, UK
[4] Present address: Faculty of Pharmacy, Hacettepe University, 06100 Ankara, Turkey
[5] To whom correspondence should be addressed. (e-mail: mhu@farmbio.uu.se)

ABBREVIATIONS: ABCB1, P-glycoprotein; $A_{tot,br}$, total (unbound, bound, intracellular) amount of drug in the brain; BBB, blood–brain barrier; CL, systemic clearance; CL_{pass}, unbound passive clearance; CL_1, clearance by influx hindrance; CL_2, clearance by efflux enhancement at the luminal membrane; CL_3, clearance by efflux enhancement at the abluminal membrane; CNS, central nervous system; CSF, cerebrospinal fluid; C_{bl}, drug concentration in blood; CL_{in}, net influx clearance; CL_{out}, net efflux clearance; $C_{u,bl}$, unbound drug concentration in blood; $C_{u,br}$, unbound drug concentration in brain; $C_{u,ec}$, unbound drug concentration in endothelium; $C_{u,ss,bl}$, unbound drug concentration in blood at steady state; $C_{u,ss,br}$, unbound drug concentration in brain at steady state; ISF, interstitial fluid; $J_{\max}$, maximal active transport capacity elimination constant; k_{el}, elimination constant; K_p, ratio of total brain to total plasma concentration; $K_{p,u}$, ratio of total brain to unbound plasma concentration; $K_{p,uu}$, ratio of unbound brain to unbound plasma concentration; K_t, unbound concentration at 50% of $J_{\max}$; M3G, morphine-3-glucuronide; M6G, morphine-6-glucuronide; OAT3, organic anion transporter; Pgp, P-glycoprotein; PS, permeability surface area; Q, mass flux; R_0, infusion rate; $t_{1/2}$, half-life; V_{bl}, vol-ume of blood in the brain tissue; $V_{u,bl}$, distribution volume of unbound drug in blood; $V_{u,br}$, distribution volume of unbound drug in brain; $V_{u,ec}$, distribution volume of unbound drug in endothelium.

INTRODUCTION

The blood–brain barrier (BBB) and its transport properties have a profound influence on the concentration–time profiles of drugs in the brain, and thereby on their central effects. The tight junctions between the endothelial cells of the BBB force all drugs to penetrate through rather than between the cells. This accentuates the differences in the passive permeabilities of lipophilic and hydrophilic drugs compared with other capillary membranes in the body. The influence of influx and efflux transporters further accentuates differences in membrane transport between drugs. In this paper, we will focus on the consequences of efflux transporters on drug concentration–time profiles in the brain. The best known and, according to current understanding, the most important efflux transporter for exogenous substances is ABCB1 (P-glycoprotein, Pgp). It is important to understand the impact of this and

other transporters on brain concentration–time profiles when developing drugs for central action, for avoidance of central side effects, or for understanding the influence of drug interactions at the BBB on the drug's central action.

To penetrate the brain tissue, the unbound drug has to pass the two membranes of the BBB endothelial cells: the luminal membrane facing the capillary blood, and the abluminal membrane facing the brain interstitial fluid (ISF). ABCB1 is present at the luminal membrane of the BBB (1). A possible action of this transporter was first described by the so-called "vacuum-cleaner model" (2–4) and more recently by the "ATP switch model" (5). These models may also serve to describe the mode of action of other luminal transporters. Because the vacuum-cleaner mode of action transports the drug back to the blood before it reaches the cytoplasm of the BBB endothelial cells (i.e., it functions as a gatekeeper, preventing influx), this process is called *influx hindrance*. An alternative mechanism for luminal efflux involves the active transport of compounds from the cytoplasm of the endothelial cells across the luminal membrane to the blood. This process results in increased efflux of substrates compared with passive transport. It is therefore referred to as *efflux enhancement*. It has been suggested that ABCB1 may act by both mechanisms (3,5–7).

Efflux transporters, such as the organic anion transporter (OAT3), are also located on the abluminal side of the BBB endothelium (8,9). In this study, we have assumed that the active process for abluminal transport is one of efflux enhancement, where drugs are taken from the brain ISF to the endothelial cell cytoplasm. It is speculated that abluminal transporters like OAT3 require assistance from a luminal transporter to extrude substances from the brain ISF all the way to the blood. To describe this situation, we have included a model combining abluminal and luminal efflux transport.

Most kinetic models of active efflux describe transport across a single membrane (10–12), but there are also some double-membrane models illustrating the uptake of glucose or other endogenous substances into the brain (13–16). Ashida *et al.* developed a model for ABCB1 based on the vacuum-cleaner mechanism, but their paper focused on cancer resistance and did not include active efflux at the BBB (17). However, they did recognize the importance of the membrane space between the vascular and intracellular compartments. Upton later developed a model similar to Ashida's, which included blood, membrane, and intracellular compartments and addressed the function of ABCB1 in the BBB (18). Around the same time, Sun *et al.* presented a comprehensive double-membrane BBB model (19). They assumed that passive transport across both membranes was symmetrical and that the drug concentration in the outer leaflets of the membranes equilibrates with that in the plasma or brain intracellular fluid, whereas the concentration in the inner leaflets equilibrates with that in the endothelial cells.

The purpose of this study was to describe the effects of the various possible efflux transport processes at the BBB on the brain concentration–time profiles of unbound drug, and the consequences for the central pharmacodynamics of the drugs. To address this question, a model was developed that comprised blood, endothelial, and brain compartments and included active transport mechanisms at different locations in the BBB as well as passive transport between the compartments.

THEORY

BBB transport comprises passive diffusion and active efflux processes (Fig. 1). The compartmentalization of the free, unbound drug in the blood, endothelial cell, and brain ISF is also described in Fig. 1. It is assumed that the equilibration between unbound and bound drug in the different compartments is not a rate-limiting process; this is also assumed for equilibration of drug between brain ISF and brain intracellular fluid and/or drug bound to components within the central nervous system (CNS). The processes are described by their clearances for passive permeation rate-limited by diffusion across the BBB and active transport out of the brain. The active processes (influx hindrance and efflux enhancement) are assumed to work according to Michaelis-Menten kinetics.

Brain ISF bulk flow and brain metabolism were not considered in the model. This assumption simplified the models without conflicting with the general aim of this paper to show the influence of different BBB processes on the brain concentration profile over time. The rate of bulk flow [0.18–0.29 μL min^{-1} (g brain)$^{-1}$ (20)] is also lower than the active efflux clearances for many drugs (21). The cerebrospinal fluid (CSF) was not included in the model. The CSF and brain compartments are separated from the vascular space by the blood–CSF barrier and the BBB, respectively. The two membranes have different permeability properties and drug concentrations in the two compartments could vary widely (22,23).

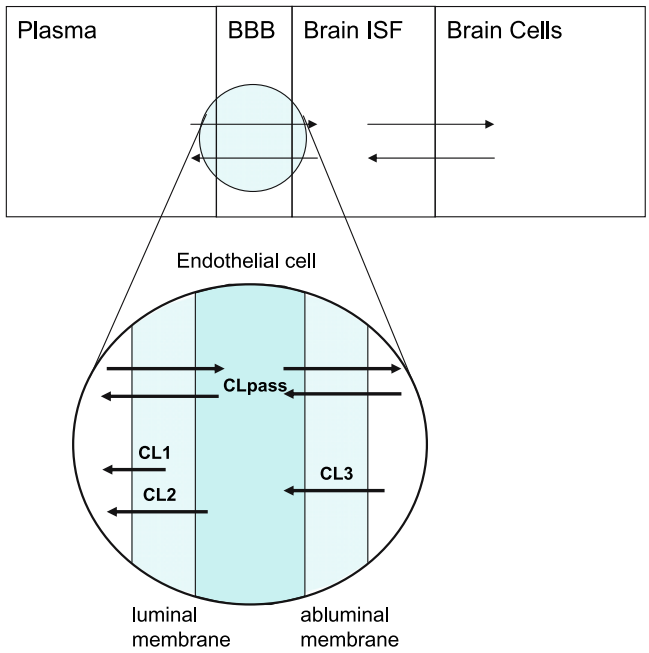

Fig. 1. The blood–brain barrier consists of endothelial cells with tight junctions. Molecules in the blood must pass two membranes before reaching the brain. The luminal membrane faces the blood and the abluminal membrane faces the brain interstitial fluid (ISF). Molecules move across the membrane barriers by passive (CL_{pass}) or active transport (CL_1, CL_2, and CL_3). CL_1 is the clearance describing influx hindrance, CL_2 is the clearance by efflux enhancement at the luminal membrane and CL_3 is the clearance by efflux enhancement at the abluminal membrane.

The Model

The model consists of passive processes in both the luminal and abluminal membranes of the endothelial cells, in combination with efflux pumps located at both membranes of the BBB (Fig. 1). It is assumed that there is instant equilibrium between the concentration of drug in the blood and that in the luminal membrane. Similarly, the concentration in the abluminal membrane is assumed to equilibrate instantly with that in the brain ISF. Therefore, the luminal membrane drug concentration is assumed to be equal to the blood concentration, and the concentration in the abluminal membrane is assumed to be equal to the concentration in the brain ISF. The passive clearance is assumed to be the same across both the luminal and abluminal membranes. The unbound drug concentrations in blood ($C_{u,bl}$), endothelium ($C_{u,ec}$), and brain ISF ($C_{u,br}$) are described by Eqs. (1)–(3). Single compartments were used for the blood, the cytosol of the endothelial cell, and the brain. Although this is a simplification for most compounds, it clarifies the consequences of the processes at the BBB on brain ISF concentration–time profiles.

$$\frac{V_{u,bl}\cdot dC_{u,bl}}{dt} = R_0 - \left(CL + CL_{pass} - CL_1\right)\cdot C_{u,bl} + \left(CL_{pass} + CL_2\right)\cdot C_{u,ec} \quad (1)$$

$$\frac{V_{u,ec}\cdot dC_{u,ec}}{dt} = \left(CL_{pass} - CL_1\right)\cdot C_{u,bl} - \left(2\cdot CL_{pass} + CL_2\right)\cdot C_{u,ec} + \left(CL_{pass} + CL_3\right)\cdot C_{u,br} \quad (2)$$

$$\frac{V_{u,br}\cdot dC_{u,br}}{dt} = CL_{pass}\cdot C_{u,ec} - \left(CL_{pass} + CL_3\right)\cdot C_{u,br} \quad (3)$$

$V_{u,bl}$, $V_{u,ec}$, and $V_{u,br}$ are the volumes of distribution of unbound drug in blood, endothelium, and brain, respectively. The infusion rate is described by R_0. In Eqs. (1)–(3), CL is the unbound systemic clearance, CL_{pass} is the unbound passive clearance across the BBB, CL_1 is the clearance by influx hindrance, i.e., the process hindering drug to reach even the cytosol of the BBB endothelial cells when drug is transported from blood. CL_2 is the clearance by efflux enhancement at the luminal membrane, i.e., transporting drug from the cytosol of the endothelial cell to blood. CL_3 is the clearance by efflux enhancement at the abluminal membrane, i.e., transporting drug from the brain ISF to the cytosol of the BBB endothelial cell. The active clearances can be defined as:

$$CL_1 = \frac{J_{\max}}{K_t + C_{u,bl}} \quad (4)$$

$$CL_2 = \frac{J_{\max}}{K_t + C_{u,ec}} \quad (5)$$

$$CL_3 = \frac{J_{\max}}{K_t + C_{u,br}} \quad (6)$$

where $J_{\max}$ is the maximal active transport capacity and K_t is the unbound concentration at 50% of $J_{\max}$.

Steady-State Brain-to-Blood Ratios

At steady state, the mass flux, Q, across the luminal endothelial membrane is given by:

$$Q = \left(CL_{pass} + CL_2\right)\cdot C_{u,ec} - \left(CL_{pass} - CL_1\right)\cdot C_{u,bl} \quad (7)$$

and that across the abluminal membrane by:

$$Q = \left(CL_{pass} + CL_3\right)\cdot C_{u,br} - CL_{pass}\cdot C_{u,ec} \quad (8)$$

Solving these two equations for $C_{u,ec}$ yields:

$$C_{u,ec} = \frac{\left(CL_{pass} + CL_3\right)\cdot C_{u,br} + \left(CL_{pass} - CL_1\right)\cdot C_{u,bl}}{2\cdot CL_{pass} + CL_2} \quad (9)$$

$C_{u,ec}$ can therefore be eliminated from Eqs. (7) and (8). By rearranging one of these equations, the following expression is obtained for Q:

$$Q = \frac{\left(CL_{pass}^2 + CL_{pass} + CL_2 + CL_{pass}\cdot CL_3 + CL_2\cdot CL_3\right)\cdot C_{u,br} + \left(CL_{pass}\cdot CL_1 - CL_{pass}^2\right)\cdot C_{u,bl}}{2\cdot CL_{pass} + CL_2} \quad (10)$$

The net influx clearance CL_{in}, sometimes also expressed as the permeability surface (PS) area product, is composed of the sum of the clearances from passive and active processes across the BBB. This is also the case for the net efflux clearance CL_{out}. Equation (10) can therefore be rewritten with the macroconstants CL_{in} and CL_{out} to describe the transport across both membranes:

$$Q = CL_{out}\cdot C_{u,br} - CL_{in}\cdot C_{u,bl} \quad (11)$$

CL_{in} and CL_{out} can therefore be defined as:

$$CL_{in} = \frac{CL_{pass}^2 - CL_{pass}\cdot CL_1}{2\cdot CL_{pass} + CL_2} \quad (12)$$

$$CL_{out} = \frac{CL_{pass}^2 + CL_{pass}\cdot CL_2 + CL_{pass}\cdot CL_3 + CL_2\cdot CL_3}{2\cdot CL_{pass} + CL_2} \quad (13)$$

Steady state occurs when mass flux is 0 [Eq. (11)], that is, when the brain-to-blood concentration ratio equals the CL_{in}-to-CL_{out} ratio. The unbound steady-state brain-to-blood concentration ratio is therefore given by:

$$\frac{C_{u,ss,br}}{C_{u,ss,bl}} = \frac{CL_{pass}^2 - CL_{pass}\cdot CL_1}{CL_{pass}^2 + CL_{pass}\cdot CL_2 + CL_{pass}\cdot CL_3 + CL_2\cdot CL_3} \quad (14)$$

Table I. Experimentally Obtained Brain Distribution Parameters for the Model Drugs

	CL (mL min^{-1})	$V_{u,br}$ [mL (g brain)$^{-1}$]	CL_{in} [μL min^{-1} (g brain)$^{-1}$]	CL_{out} [μL min^{-1} (g brain)$^{-1}$]	Brain/blood unbound concentration ratio ($K_{p,uu}$)	Reference
M3G	4.5	0.23	0.11	1.2	0.10	(28)
M6G	9.8	0.29	1.7	5.7	0.29	(30)
Morphine	28	1.7	11	42	0.27	(31)
Gabapentin	–	5.5	44	380	0.12	(32)

The ratio of the steady-state concentrations of unbound drug in brain and blood $C_{u,ss,br}/C_{u,ss,bl}$ [Eq. (14)] is equal to the partition coefficient of unbound drug in brain and blood, $K_{p,uu}$. In situations involving only passive transport, CL_1, CL_2, and CL_3 are equal to 0 and $K_{p,uu}$ will be 1. CL_2 and CL_3 are 0 when the active pump works by influx hindrance only and Eq. (14) can be simplified to $K_{p,uu} = 1-(CL_1/CL_{pass})$. When the active pump works by efflux enhancement at the luminal membrane (CL_1 and CL_3 are 0), $K_{p,uu} = 1/[1 + (CL_2/CL_{pass})]$. And finally, when the active pump works by efflux enhancement at the abluminal membrane (CL_1 and CL_2 are 0), $K_{p,uu} = 1/[1 + (CL_3/CL_{pass})]$. The same holds for the situation when two pump functions are working together. CL_3 is 0 when influx hindrance and efflux enhancement are working together at the luminal membrane. Then $K_{p,uu} = (CL_{pass} - CL_1)/(CL_{pass} + CL_2)$. CL_1 is 0 when efflux enhancement is active at both the luminal and abluminal membranes and $K_{p,uu} = CL_{pass}^2/[CL_{pass}^2 + (CL_{pass} \times CL_2) + (CL_{pass} \times CL_3) + (CL_2 \times CL_3)]$.

Model Substances

Experimentally obtained values were used as a basis for extrapolation of the contribution of passive and active processes on the net CL_{in} and CL_{out} in the simulation model. Previously reported net influx and efflux clearances (CL_{in}, CL_{out}) for M3G, M6G, morphine, and gabapentin are shown in Table I. Possible passive and active clearances for the four model substances were estimated by solving Eqs. (12) and (13) for a situation in which one of the three suggested processes is active. For the situation with only influx hindrance:

$$CL_1 = 2 \cdot (CL_{in} - CL_{out}) \quad (15)$$

$$CL_{pass} = 2 \cdot CL_{out} \quad (16)$$

For the situation with efflux enhancement at the luminal membrane:

$$CL_2 = \frac{CL_{out}^2 - CL_{in}^2}{CL_{in}} \quad (17)$$

$$CL_{pass} = CL_{out} + CL_{in} \quad (18)$$

For the situation with efflux enhancement at the abluminal membrane:

$$CL_3 = 2 \cdot (CL_{out} - CL_{in}) \quad (19)$$

$$CL_{pass} = 2 \cdot CL_{in} \quad (20)$$

The estimates of passive and active clearances for these three situations and the four model substances are shown in Table II. The ratio of the rate of specific active efflux to that of passive transport (CL_1/CL_{pass}, CL_2/CL_{pass}, CL_3/CL_{pass}) illustrates the efficiency of that specific type of transport in sustaining the equilibrium across the BBB found experimentally, given that that transport process is the only one acting on the drug.

SIMULATION SETUP

Simulations were carried out to elucidate the role of the various efflux clearance mechanisms. The systems of differential equations were solved using Laplace transforms. The concentration–time profiles in the three compartments were then simulated using MATLAB 6.5 (24).

The rat was used as a model because much experimental data for this species are available for comparison with the simulations. In the first set of simulations, it was assumed that the compounds were uniformly distributed throughout the body, and the physiological volumes of total body water (167 mL) and brain [0.7 mL (g brain)$^{-1}$] in rats were used as

Table II. Estimated Active and Passive Clearances [μL min^{-1} (g brain)$^{-1}$] and Ratios between Active and Passive Clearances for the Model Drugs

	Influx hindrance (luminal)[a]			Efflux enhancement (luminal)[b]			Efflux enhancement (abluminal)[c]		
	CL_1	CL_{pass}	CL_1/CL_{pass}	CL_2	CL_{pass}	CL_2/CL_{pass}	CL_3	CL_{pass}	CL_3/CL_{pass}
M3G	2.1	2.3	0.90	12	1.3	9.5	2.1	0.2	9.5
M6G	8.0	11	0.71	18	7.3	2.4	8.0	3.3	2.4
Morphine	61	84	0.73	140	53	2.7	61	23	2.7
Gabapentin	660	750	0.88	3200	420	7.5	660	88	7.5

[a] Values were calculated based on CL_{in} and CL_{out} from Table I and Eqs. (15) and (16).
[b] Values were calculated based on CL_{in} and CL_{out} from Table I and Eqs. (17) and (18).
[c] Values were calculated based on CL_{in} and CL_{out} from Table I and Eqs. (19) and (20).

volumes of distribution in the blood and brain compartments, respectively (25). A value of 0.8 μL (g brain)$^{-1}$ was assigned as the volume of brain endothelial cells (14,26).

The body clearance (CL) was set to 5 mL min^{-1}, resulting in an elimination constant (k_{el}) out of the body of 0.03 min^{-1} and a half-life of 23 min. The unbound drug concentration in the blood was set to steady state ($C_{u,ss,bl}$) at time = 0 to clarify the time for equilibration across the BBB. The infusion rate (R_0) was equal to $C_{u,ss,bl} * CL$ to maintain steady-state concentrations with an infusion time of 8 h. The simulations were continued for a further 8 h following the end of the infusion. Relatively long times were used so as to follow the concentrations of poorly permeable model compounds.

CL_{pass} values of 0.3, 3, 10, 30, and 300 μL min^{-1} (g brain)$^{-1}$ were used in the simulations (Table III). Increasing CL_{pass} values are associated with increasingly lipophilic physicochemical properties. Two different J_{max} values [5 and 10 ng min^{-1} (g brain)$^{-1}$] and one K_t value (1000 ng mL^{-1}) were investigated in the simulations. These results in CL_1, CL_2, and CL_3 maximum values of 5 or 10 μL min^{-1} (g brain)$^{-1}$. At steady state, the active clearances are somewhat lower, because the denominator of the Michaelis-Menten ratio [Eqs. (4)–(6)] includes the concentration that drives the efflux pumps. These active and passive clearances cover the range displayed by the model substances (M3G, M6G, morphine, and gabapentin) (Table II). The $C_{u,ss,bl}$ level was set to 200, i.e., much smaller than K_t, to perform the simulations in the linear range of the active transport capacity. A CL_{pass} of 10 or 30 μL min^{-1} (g brain)$^{-1}$ was chosen for presentation in the figures. A summary of simulation parameter values is given in Table III.

The unbound volume of distribution in brain ($V_{u,br}$ in milliliters per gram brain) is a direct description of how drugs are distributed within the brain, independent of the BBB transport:

$$V_{u,br} = \frac{A_{tot,br} - V_{bl} * C_{bl}}{C_{u,br}} \quad (21)$$

$A_{tot,br}$ is the total (unbound, bound, intracellular, etc.) amount of drug in the brain, V_{bl} is the volume of blood in the brain tissue, and C_{bl} is the concentration of drug in the blood. The volume fraction ($V_{u,br}$) for ions (cation tetramethylammonium and anion α-napthalenesulphonate) of 0.2 mL (g brain)$^{-1}$ (27), was taken as the brain ISF volume. Values close to 1 mL (g brain)$^{-1}$ describe an even distribution throughout the whole brain tissue. Values above 1 mL (g brain)$^{-1}$ describe an affinity for brain tissue and probable intracellular distribution. The influence of the volume of distribution in the brain on the brain concentration profiles was therefore investigated in a second set of simulations in which the other parameters were kept constant (Table IV). The $V_{u,br}$ was first set to 0.2 mL (g brain)$^{-1}$, aiming to describe distribution solely into the brain ISF. This value is very close to the volume of distribution in brain reported for unbound M3G (28) and M6G (29,30). Increasing $V_{u,br}$ values to 2, 5, and 10 mL (g brain)$^{-1}$ were then studied in the simulations to cover the values of 1.7 mL (g brain)$^{-1}$ reported for morphine (31) and 5.5 mL (g brain)$^{-1}$ reported for gabapentin (32). A summary of simulation parameter values with varied $V_{u,br}$ is given in Table IV.

The units for clearance used in the MATLAB simulations were milliliters per minute. Therefore, clearances and volumes given above in microliters per minute per gram brain, milliliters per gram brain, and microliters per gram brain were recalculated to accommodate the whole organ weight by multiplication by the weight of the average rat brain (1.8 g) (25).

The half-life ($t_{1/2}$) of the drug in the brain was calculated from the simulated slopes during the elimination phase (Figs. 2–9, Table V). This value can be approximated to $t_{1/2} = V_{u,brain} \times CL_{out}$.

Table III. Summary of Simulation Parameters when CL_{pass} and J_{max} were Varied

Parameters varied	
CL_{pass}	0.3, 3, 10, 30, 300 μL min^{-1} (g brain)$^{-1}$
J_{max}	5, 10 ng min^{-1} (g brain)$^{-1}$
Parameters kept constant	
CL	5 mL min^{-1}
$C_{u,ss,bl}$	200 ng mL^{-1}
K_t	1000 ng mL^{-1}
$V_{u,bl}$	167 mL
$V_{u,ec}$	0.8 μL (g brain)$^{-1}$
$V_{u,br}$	0.7 mL (g brain)$^{-1}$
Infusion time	8 h
Elimination time	8 h

Table IV. Simulation Parameters when $V_{u,br}$ was Varied

Parameters varied	
$V_{u,br}$	0.2, 0.7, 2, 5, 10 mL (g brain)$^{-1}$
Parameters kept constant	
CL	5 mL min^{-1}
CL_{pass}	10 μL min^{-1} (g brain)$^{-1}$
$C_{u,ss,bl}$	200 ng mL^{-1}
J_{max}	10 ng min^{-1} (g brain)$^{-1}$
K_t	1000 ng mL^{-1}
$V_{u,bl}$	167 mL
$V_{u,ec}$	0.8 μL (g brain)$^{-1}$
Infusion time	8 h
Elimination time	8 h

RESULTS

Figure 2 shows the uptake of drug into the brain at various passive permeabilities. As expected, decrease in CL_{pass} results in decrease in transport rates into the brain and a longer time to reach steady-state levels in the brain. Eventually, the same steady-state unbound drug concentration in blood and brain ISF is reached, i.e., $K_{p,uu}$ is 1, independently of the magnitude of the passive clearance. For highly permeable drugs, when CL_{pass} is high, the brain concentration–time profiles are almost parallel to the blood concentration–time profiles and, hence, the same half-life is observed in blood and brain. When CL_{pass} is lower, the half-life in brain is longer because of slower redistribution between brain and blood.

The effect on the brain profile of influx hindrance and efflux enhancement at the luminal membrane is shown in

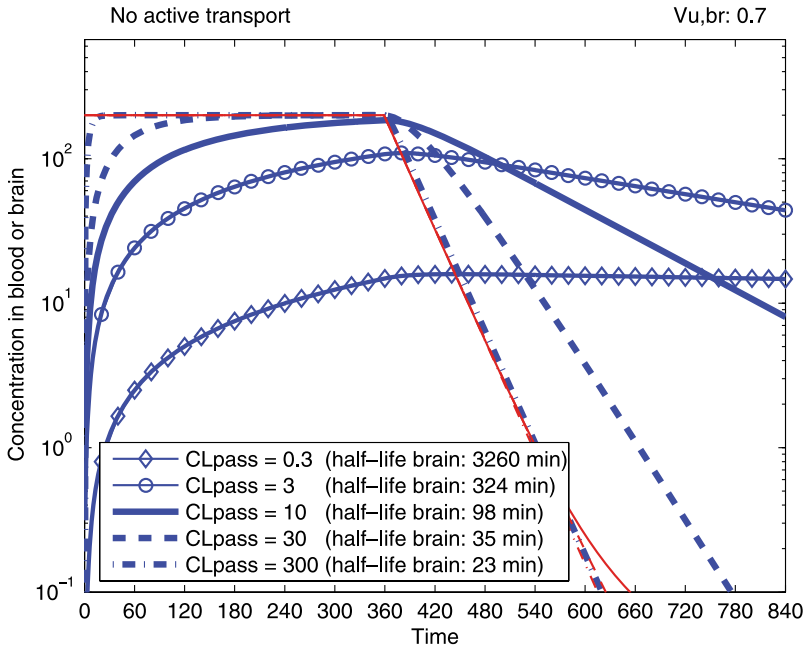

Fig. 2. Representation of the effect of various values of CL_{pass} on the brain concentration–time profiles when no active transport mechanism is present. When given as a constant venous infusion, a compound with a lower CL_{pass} will take longer to reach steady state than a compound with a higher CL_{pass}. However, they will both have the same unbound concentration in blood and brain ISF when steady state is eventually reached. A lower CL_{pass} will also result in a longer half-life in the brain. The thin lines describe the unbound concentration in blood with the respective type of active transports.

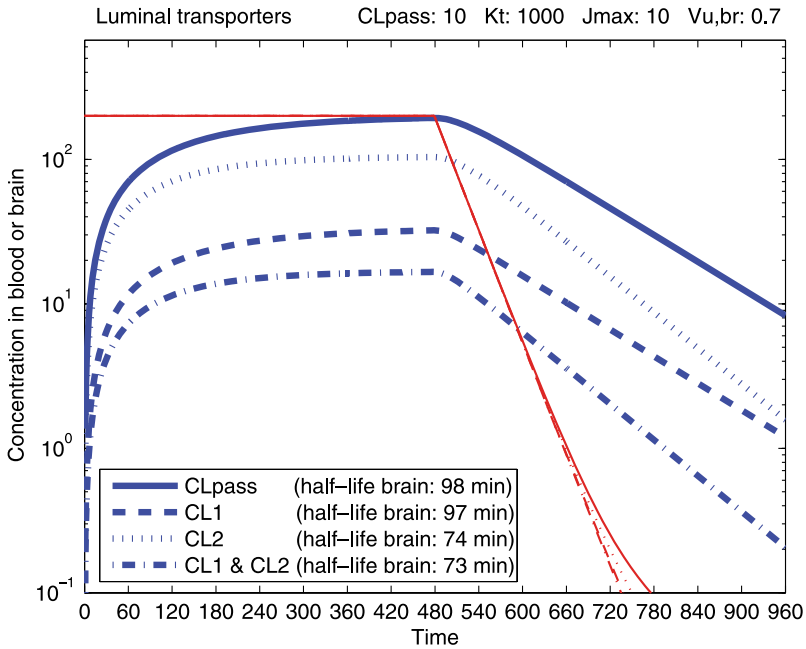

Fig. 3. Representation of the effect of active transport at the luminal membrane on brain concentration–time profiles. Influx hindrance (CL_1) is more effective in decreasing drug concentrations in the brain than efflux enhancement (CL_2) at this membrane. The combination of both active processes (CL_1 & CL_2) results in a brain-to-blood ratio of unbound drug concentrations similar to the product of the ratios for the two separate processes. Efflux enhancement results in a shorter half-life in the brain than that seen with passive transport alone (CL_{pass}), whereas influx hindrance does not affect the half-life in the brain. The thin lines describe the unbound concentration in blood with the respective type of active transports.

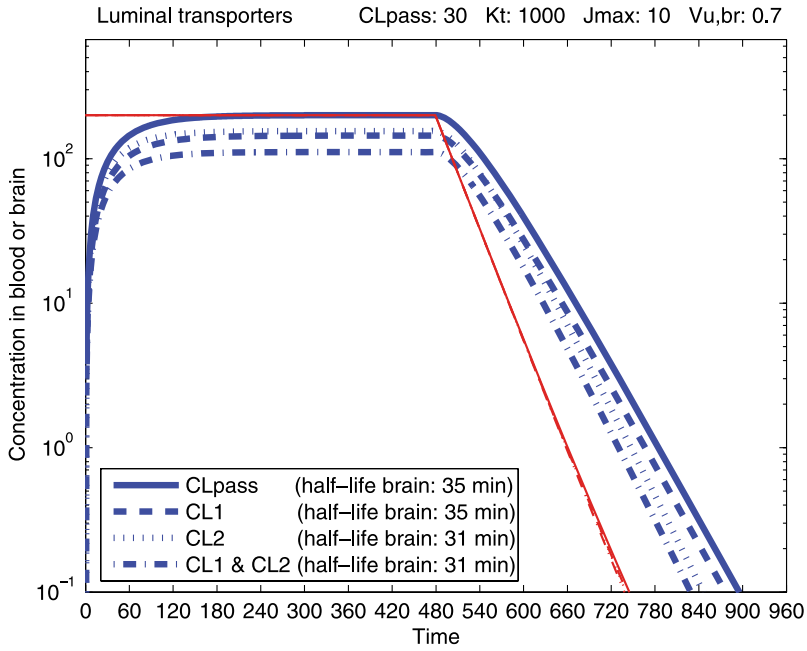

Fig. 4. Representation of the effect of increased drug lipophilicity (i.e., increased CL_{pass}) on brain concentrations (compared with Fig. 3). The active transport processes have a less profound influence on the brain concentration profiles for drugs with higher lipophilicity. (Nonetheless, the capacity of the active efflux process remains unchanged). The thin lines describe the unbound concentration in blood with the respective type of active transports.

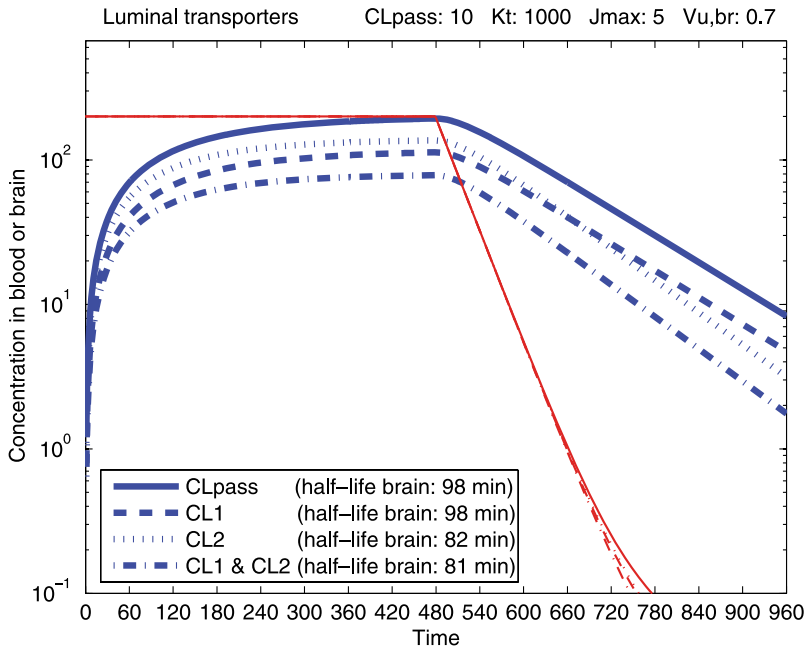

Fig. 5. Representation of the effect of drugs with decreased active transport capacity, J_{max}, on brain concentrations (compared with Fig. 3). The brain-to-blood ratio of unbound drug concentrations at steady state is increased when J_{max} is lower. Higher J_{max} values correspond to increased active transport (increased CL_1 and/or CL_2). The thin lines describe the unbound concentration in blood with respective type of active transports.

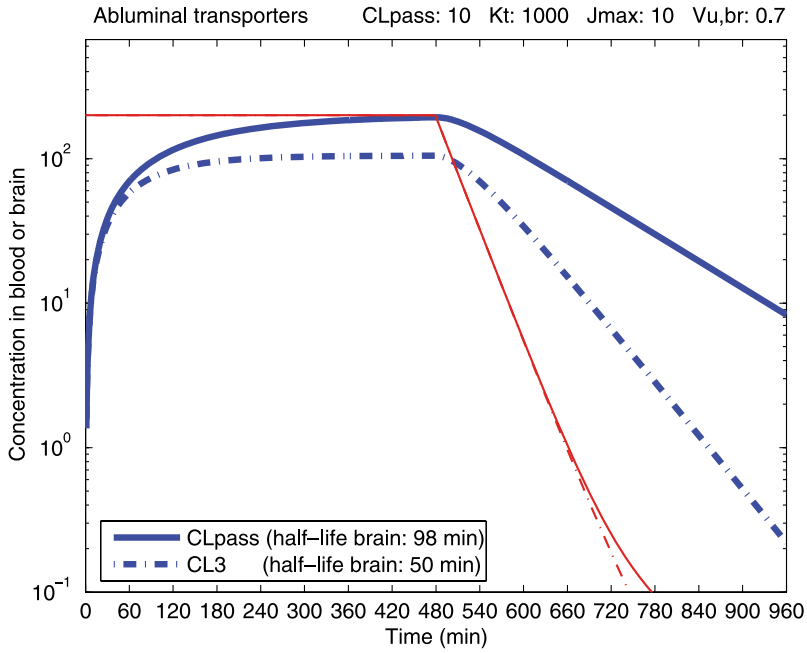

Fig. 6. Representation of the effect of active transport at the abluminal membrane on the brain concentration–time profiles. Efflux enhancement at the abluminal membrane (CL_3) results in a brain-to-blood ratio of unbound drug concentrations the same as that obtained for efflux enhancement on the luminal side (Fig. 3). The time to steady state in the brain and the half-life are shorter than those in the luminal model (Fig. 3). The thin lines describe the unbound concentration in blood with the respective type of active transports.

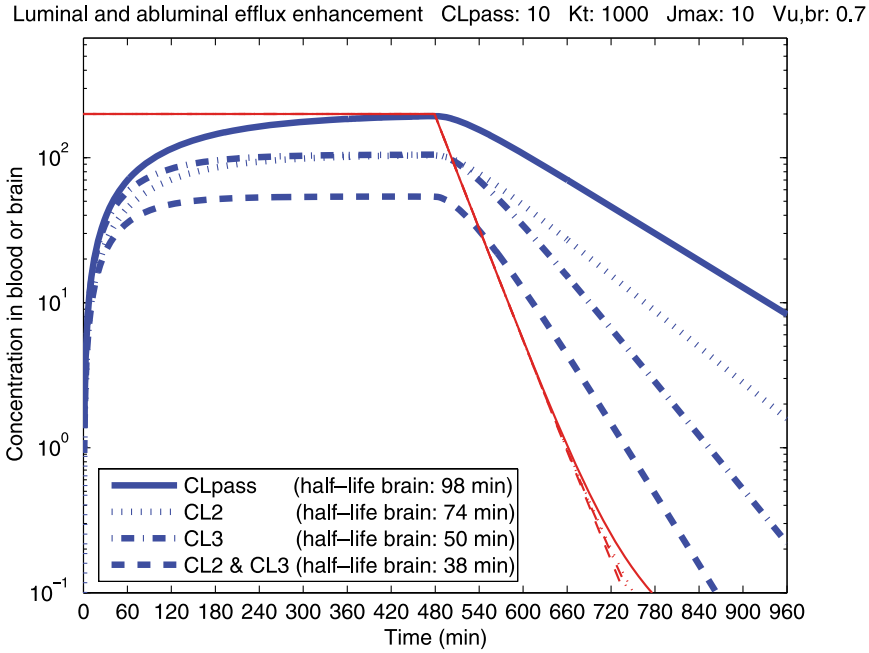

Fig. 7. Representation of efflux enhancement at both luminal and abluminal membranes. The combination of the two active processes (CL_2 & CL_3) results in a brain-to-blood ratio of unbound drug concentrations similar to the product of the ratios for the two separate processes. The effect on the brain-to-blood ratio of unbound drug concentrations is similar to that seen with influx hindrance (Fig. 3). The thin lines describe the unbound concentration in blood with the respective type of active transports.

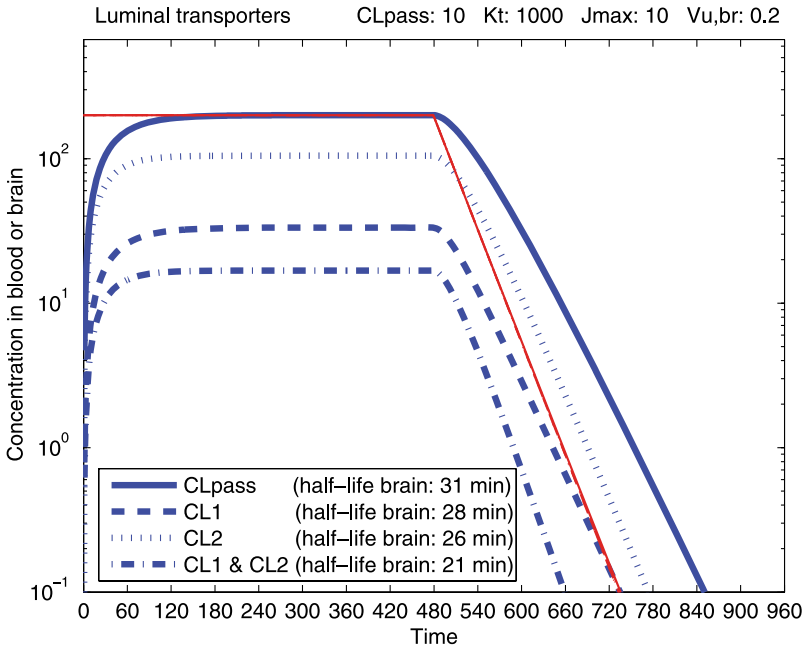

Fig. 8. Representation of the effect of drugs with a lower unbound volume of distribution [0.2 mL (g brain)$^{-1}$] in the brain, $V_{u,br}$, than represented in Fig. 3. The brain-to-blood ratio of unbound drug concentrations at steady state is not affected by the decreased $V_{u,br}$. The time to steady state and the half-life in the brain are, however, shorter. The thin lines describe the unbound concentration in blood with respective type of active transports.

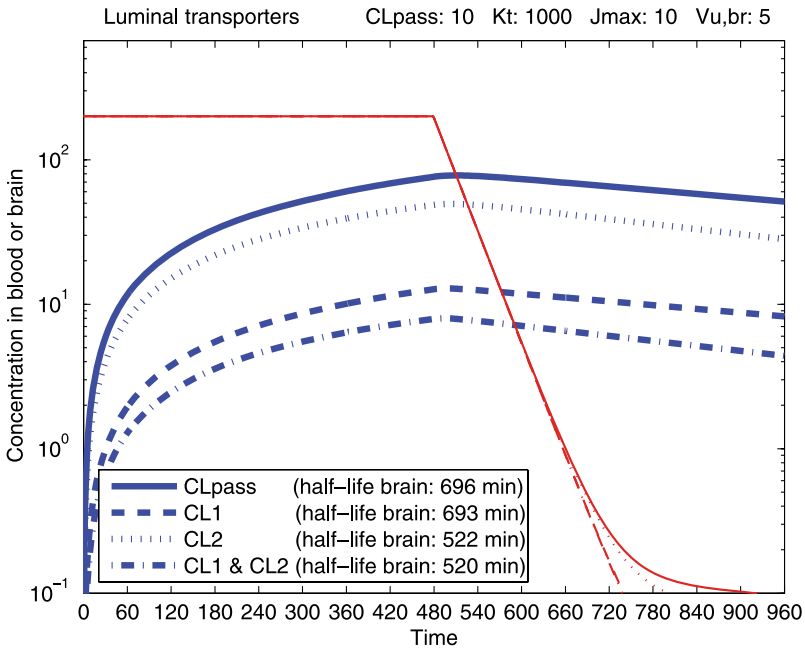

Fig. 9. Representation of the effect of drugs with a higher unbound volume of distribution [5 mL (g brain)$^{-1}$] in the brain, $V_{u,br}$, than represented in Fig. 3. The brain-to-blood ratio of unbound drug concentrations at steady state is not affected by the increased $V_{u,br}$. The time to steady state and the half-life in the brain are, however, longer; steady state will not be reached during the 8-h constant infusion. The thin lines describe the unbound concentration in blood with the respective type of active transports.

Table V. Brain-to-Blood Ratios of Unbound Drug Concentrations ($K_{p,uu}$) and Half-lives in Brain

CL_{pass}[a]	No active transport	CL_1[b]		CL_2[b]		CL_1 and CL_2[b]		CL_3[b]		CL_2 and CL_3[b]	
		5	10	5	10	5	10	5	10	5	10
Brain-to-blood unbound concentration ratio ($K_{p,uu}$)											
0.3	1[c]	–	–	0.06[c]	0.03[c]	–	–	0.06	0.03	0.003	0.001
3	1[c]	–	–	0.39[c]	0.24[c]	–	–	0.39	0.24	0.15	0.06
10	1	0.58	0.17	0.69	0.52	0.40	0.08	0.69	0.52	0.48	0.27
30	1	0.86	0.72	0.88	0.78	0.75	0.56	0.88	0.78	0.77	0.60
300	1	0.99	0.97	0.99	0.97	0.97	0.95	0.99	0.97	0.97	0.95
Half-life in brain (min)											
0.3	3200	–	–	1700	1700	–	–	190	96	97	50
3	320	–	–	220	200	–	–	120	76	84	47
10	98	98	97	82	74	81	73	66	50	55	38
30	35	35	35	33	31	33	31	31	28	29	26
300	23	23	23	23	23	23	23	23	23	23	23

The active clearances (CL_1, CL_2, and CL_3) are given at their maximum value. CL was set to 5 mL min^{-1}, K_t to 1000 ng mL^{-1}, $V_{u,bl}$ to 167 mL, $V_{u,ec}$ to 0.8 μL (g brain)$^{-1}$, and $V_{u,br}$ to 0.7 mL (g brain)$^{-1}$.
[a] Passive clearance [μL min^{-1} (g brain)$^{-1}$].
[b] Maximum active efflux (J_{max}/K_t) [μL (min g brain)$^{-1}$]. At steady state the active clearances are somewhat lower, as the Michaelis-Menten ratio $J_{max}/(K_t + C_u)$ includes the concentration that drives the efflux pumps.
[c] The steady-state ratios presented here are obtained using Eq. (14). The ratios obtained in the simulations with low CL_{pass} rates were lower than those obtained using Eq. (14) because steady state was not reached within the 8-h infusion time.

Fig. 3. The influx hindrance process, using CL_1, is more effective in decreasing brain concentrations than efflux enhancement, using CL_2. A combination of both CL_1 and CL_2 is the most effective. Under the simulation conditions used in Fig. 3 [CL_{pass} of 10 μL min^{-1} (g brain)$^{-1}$ and J_{max} of 10 ng min^{-1} (g brain)$^{-1}$] the $K_{p,uu}$ was 0.17 for influx hindrance, 0.52 for efflux enhancement, and 0.08 for both processes working together. The $K_{p,uu}$ value for both processes together is similar to the product of the $K_{p,uu}$ values for the separate processes ($0.17 \times 0.52 = 0.09$) (Table V). However, it may be more accurate to compare the situation using CL_1 at a capacity (J_{max}) of 10 ng min^{-1} (g brain)$^{-1}$ with the situation using CL_1 and CL_2 at capacities of 5 μL min^{-1} (g brain)$^{-1}$ for each, because the two mechanisms would then have the combined capacity of 10 μL min^{-1} (g brain)$^{-1}$. In that case, influx hindrance is more effective than the combination of CL_1 and CL_2. The $K_{p,uu}$ at a CL_{pass} of 10 μL min^{-1} (g brain)$^{-1}$ was 0.17 for influx hindrance alone and 0.40 for the combination of influx hindrance and efflux enhancement (Table V). Efflux enhancement decreased the drug half-life in brain compared with passive transport alone, whereas influx hindrance had no effect on the half-life in the brain (Table V). This can be explained by Eq. (13). In the situation with only passive clearance, the CL_{out} rate is half the $CL_{passive}$ rate. This is also true for the situation with both influx hindrance and passive clearance. Hence, the transport of drug from the brain back to the blood is not dependent on any active efflux mechanism in either situation. For drugs affected by efflux enhancement, the CL_{out} expression includes CL_2 and the clearance will therefore differ from the passive clearance. Efflux enhancement will therefore reduce the half-life of drug in the brain compared with the passive situation.

The active and passive clearances of the four model substances also indicate that influx hindrance is the most efficient mechanism (Table II). CL_2 and CL_3 would have to be several times higher than CL_1 to result in the same $K_{p,uu}$. In fact, CL_1 must be lower than CL_{pass} for any drug to penetrate the brain. Efflux enhancement rates, CL_2 or CL_3, on the other hand, can be much higher (9.5 times for M3G) than CL_{pass} and still result in drug uptake into the brain. This can also be seen in Table V.

Table VI. Half-Life in Brain at Varying Volumes of Distribution in the Brain ($V_{u,br}$)

$V_{u,br}$[a]	Half-life in brain (min)					
	No active transport	CL_1[b] 10	CL_2[b] 10	CL_1 and CL_2[b] 10	CL_3[b] 10	CL_2 and CL_3[b] 10
0.2	31	28	26	21	23	23
0.7	98	97	74	73	50	38
2	280	280	210	210	140	110
5	700	700	520	520	350	260
10	1400	1400	1000	1000	710	530

CL was set to 5 mL min^{-1}, CL_{pass} to 10 μL min^{-1} (g brain)$^{-1}$, K_t to 1000 ng mL^{-1}, $V_{u,bl}$ to 167 mL, and $V_{u,ec}$ to 0.8 μL (g brain)$^{-1}$.
[a] Volume of distribution of unbound drug in the brain [μL (g brain)$^{-1}$].
[b] Maximum active efflux (J_{max}/K_t) [μL (min g brain)$^{-1}$]. At steady state, the active clearances are somewhat slower, as the Michaelis-Menten ratio $J_{max}/(K_t + C_u)$ includes the concentration that drives the efflux pumps.

In Fig. 4, the CL_{pass} rate is 30 μL min^{-1} (g brain)$^{-1}$, instead of 10 μL min^{-1} (g brain)$^{-1}$ (Fig. 3). The figure demonstrates the perhaps obvious fact that the influence of the active processes on the brain time–concentration profiles decreases with increasing lipophilicity, given the same active process capacity.

The maximal active transport capacity in Fig. 5 [J_{max} = 5 ng min^{-1} (g brain)$^{-1}$] is lower than that in Fig. 3 [J_{max} = 10 ng min^{-1} (g brain)$^{-1}$]. The $K_{p,uu}$ at steady state in this case was higher than that in Fig. 3. Although the half-life for the influx hindrance process remained the same when J_{max} was decreased, the half-life for efflux enhancement increased (Table V).

Simulated drug profiles where an efflux pump is active at the abluminal membrane are shown in Fig. 6. Efflux enhancement on the abluminal side of the BBB resulted in a $K_{p,uu}$ equal to that for the same process on the luminal side, but the time to steady state and the half-life in the brain were lower than those in the luminal model (Table V). Equation (14) shows that the ratio of brain to blood concentrations of unbound drug, $K_{p,uu}$, will be the same for efflux enhancement regardless of whether it is present at the luminal or the abluminal membrane. Equation (13) shows that CL_2 occurs in both the denominator and the numerator of the CL_{out} expression. CL_3, however, is only found in the numerator. Hence, Eq. (14) explains why the same $K_{p,uu}$ is obtained for CL_2 and CL_3 when they are of the same magnitude. Similarly, Eq. (13) explains why the half-life is different in these two situations.

Finally, the influence of two pumps working by the efflux enhancement mechanism at both the luminal and abluminal membrane was studied. The profiles are shown in Fig. 7. Efflux enhancement at both membranes reduced $K_{p,uu}$ to a value similar to the product of the separate processes ($0.52 \times 0.52 = 0.27$). The half-life in brain was shorter than those in situations with only CL_1, only CL_2, only CL_3, or CL_1 and CL_2 together. For low CL_{pass} rates [(up to 10 μL min^{-1} (g brain)$^{-1}$], the combination of efflux enhancement at both membranes was less effective than influx hindrance alone at the luminal membrane (CL_1) in reducing brain concentrations. For higher CL_{pass} rates, the combination of CL_2 and CL_3 was more effective than CL_1 alone, but was never as effective as CL_1 in combination with CL_2 (Table V).

Figures 8 and 9 show the influence on the brain concentration profiles of decreased and increased brain volumes of distribution ($V_{u,br}$) compared with those in Fig. 3. A drug with a small volume of distribution in the brain will have a shorter half-life in the brain than a drug with a large volume of distribution, when all other parameters such as CL_{pass} and J_{max} are the same for both drugs (Table VI). The $K_{p,uu}$ is not dependent on volume of distribution [Eq. (14)].

DISCUSSION

The purpose of this study was to provide more insight into the interplay between the passive permeability properties of a drug, the active efflux mechanisms of BBB transport, and the drug concentration–time profile in the brain.

The simulated concentrations in the luminal and abluminal membranes were set equal to those in the blood and brain ISF, respectively (Fig. 1). This is clearly a simplification, as it is very unlikely that the concentration over the whole membrane will be the same. It is, however, very difficult to estimate the concentration profiles in these membranes. The concentration could change exponentially from a concentration in the outer part of the membrane that is similar to that in the blood or brain ISF to a concentration in the inner part of the membrane that is similar to that in the endothelial cells. The drug could also accumulate in the membranes, with resultant concentrations higher than those both outside and inside the endothelial cells. The magnitude of the active clearances used in this work is dependent on the local concentrations at the transporter sites.

The efficiency of the influx hindrance mechanism might be the reason for the location of ABCB1 at the luminal membrane as a protector of brain function. The luminal location of ABCB1 is probably due to the evolutionary advantage of being able to effectively exclude exogenous compounds from the brain. Active efflux on the luminal side of the BBB will not effectively transport endogenously produced substances in the brain, i.e., homovanillic acid, to the blood. Efflux mechanisms are, therefore, also needed at the abluminal membrane, perhaps in combination with an efflux enhancement transporter on the luminal side (9,33).

Golden and Pollack, who simulated the influence on brain drug profiles of blocking active transport (11), achieved similar results to those reported here. They showed that inhibition of influx hindrance will increase brain concentrations more effectively than inhibition of efflux enhancement. Assuming that there is only one transporter for each drug, complete inhibition of that particular transporter will result in a concentration–time profile the same as that for passive transport alone. Thus, the difference between the passive profile and the profile under active efflux is related to a "Pgp effect" (34). The Pgp effect was experimentally defined as the ratio of the permeabilities to a specific drug (CL_{in}) in Pgp knockout mice and wild-type mice (34). Although these authors compare permeability properties, we have compared the steady-state ratio of brain to plasma concentrations of unbound drug, $K_{p,uu}$, across the BBB. These comprise two different measurements of active efflux. When there is only influx hindrance (CL_1), the result will be the same for the Pgp effect (based on permeability) and the steady-state ratios [Eq. (12)]. However, the two methods will not give the same result for efflux enhancement because CL_{in} and the brain-to-blood steady-state ratio change to different extents when CL_2 and CL_3 are present [Eqs. (12) and (14)].

The permeability clearance of the BBB to unbound drug, i.e., the net influx clearance [Eq. (12)], does not solely *per se* control the steady-state brain concentration of the unbound drug or $K_{p,uu}$. At steady state, the $K_{p,uu}$ will equal CL_{in}/CL_{out}. Both CL_{in} and CL_{out}, however, are dependent on passive as well as active transport [Eqs. (12) and (13)]. It is the relationship between the passive clearance and the effectiveness of the efflux system (J_{max}/K_t) that defines $K_{p,uu}$. A lipophilic compound with a high passive clearance in combination with an efficient efflux system might have exactly the same $K_{p,uu}$ as a more hydrophilic compound with a low passive clearance and a less efficient efflux system. However, the time needed to attain this concentration will be different and will depend on CL_{out} and $V_{u,br}$.

The extent of active efflux will be determined by the ratio between J_{max} and K_t in combination with the local drug concentration at the transporter site. The effect of active transport on the concentration of unbound drug in the brain is most profound for systems with a high J_{max}-to-K_t ratio. This was also shown earlier by Oyler *et al.* (16). To date, there have not been many J_{max} and K_t values reported for active efflux transporters. However, Takanaga *et al.* (35) and Cisternino *et al.* (36) have reported J_{max} and K_t values resulting in similar ratios to those we have used in this paper.

Influx hindrance resulted in similar half-lives in brain to those seen with passive clearance alone (Table V). Efflux enhancement, on the other hand, resulted in shorter half-lives in the brain. Inhibition experiments can therefore give an indication of the type of active efflux that is present at the BBB; if the half-life of a drug in the brain is unchanged when an inhibitor is given, it is likely that the drug is effluxed through an influx hindrance mechanism and, if the brain half-life is increased, it is likely that the drug is effluxed through an efflux enhancement mechanism (28,31).

The same pharmacokinetic rules apply to the brain as to the body. Thus, the volume of distribution of unbound drug in the brain will not influence the steady-state $K_{p,uu}$. Neither the influx nor the efflux clearance is dependent on brain distribution. The half-life in the brain is, in parallel to plasma half-life, dependent on both the volume of distribution in the brain and the efflux clearance. Hence, compounds with very different $V_{u,br}$ values might have the same $K_{p,uu}$ but different half-lives in the brain. The timing of effects within the CNS will therefore be different.

In this paper, we have addressed the concentrations in the ISF of unbound model drugs. The total brain concentrations are in general used to give a ratio of total brain to total plasma concentration (K_p) or total brain to unbound plasma concentration ($K_{p,u}$). The ratio of unbound drug concentration in the brain to that in blood ($K_{p,uu}$) describes the effectiveness of the active efflux process at the BBB. With effective efflux systems, it is unlikely that the total concentration ratio (K_p) will be higher than unity, but this could occur if the drug is extensively bound to brain tissue. The K_p or $K_{p,u}$ ratios will be higher than the $K_{p,uu}$ ratios for drugs with a high affinity for brain tissue, thus masking the influence of active efflux. Gabapentin, with a $V_{u,br}$ of 5.5 mL (g brain)$^{-1}$, a $K_{p,uu}$ of 0.12, and a K_p of 0.7, is such an example (32). In comparison, M3G has a $V_{u,br}$ of 0.23 mL (g brain)$^{-1}$, a $K_{p,uu}$ of 0.10, and a K_p of only 0.05.

For a very hydrophilic, poorly permeable molecule, several days of constant infusion is necessary to reach steady-state concentrations in the brain, whereas a more lipophilic molecule will reach steady state much more quickly. Similarly, a molecule with a large volume of distribution in the brain will reach a new steady state more slowly than a molecule with a small volume of distribution. However, all molecules that are unaffected by active efflux will have a $K_{p,uu}$ of 1. This does not take the bulk flow into account, which might influence the efflux clearance of hydrophilic compounds to a significant extent. Hence, a hydrophilic molecule will have good central effects if it is not effluxed actively; it is just a question of the time required to reach therapeutic concentrations in the brain. If it is possible to wait until steady state is reached, these drugs should not be discarded from clinical use just because of a low uptake rate. Morphine and M6G, for example, both have the same $K_{p,uu}$ in spite of a 10-fold difference in permeability clearance (CL_{in}), and both are clinically active.

The uptake of drugs into the brain is associated with two distinct issues: the *rate* of uptake and the *extent* of uptake. The uptake rate is dependent on the physicochemical properties of the molecule, such as hydrophilicity, as well as on the involvement of active efflux. The uptake extent (at steady state), i.e., the $K_{p,uu}$, is only dependent on the involvement of active efflux at the BBB if brain metabolism and bulk flow are negligible. We suggest that as yet undiscovered transport systems exist for hydrophilic compounds and that these molecules are being effluxed to a much greater extent than is currently believed. One example in support of this theory is the previously mentioned homovanillic acid (9). Another example could be hydoxyurea, a hydrophilic substance that is believed to be effluxed by a probenecid-sensitive efflux system (37).

CONCLUSIONS

This study investigated three types of active efflux processes at the BBB: influx hindrance at the luminal membrane, and efflux enhancement at the luminal and abluminal membranes. Influx hindrance is the most effective of these processes for lowering brain concentrations of drug molecules. Furthermore, efflux enhancement decreases the half-life of the drug in brain, whereas influx hindrance does not alter the half-life from that seen with passive transport alone. The brain-to-blood ratios of unbound drug concentrations at steady state, $K_{p,uu}$, will be less than unity when steady state is reached if the molecule is being actively effluxed. The volume of distribution of unbound drug in the brain will not influence $K_{p,uu}$ and is not influenced by the permeability of the BBB to that drug *per se*. However, the time required to reach steady state for more poorly permeable drugs may be excessive from a therapeutic perspective.

ACKNOWLEDGMENTS

This work was supported by the Swedish foundation for strategic research (Stockholm, Sweden), by the Swedish Research Council no 11558, and by Uppsala Imanet (Uppsala, Sweden).

REFERENCES

1. A. Tsuji, T. Terasaki, Y. Takabatake, Y. Tenda, I. Tamai, T. Yamashima, S. Moritani, T. Tsuruo, and J. Yamashita. P-glycoprotein as the drug efflux pump in primary cultured bovine brain capillary endothelial cells. *Life Sci.* **51**:1427–1437 (1992).
2. Y. Raviv, H. B. Pollard, E. P. Bruggemann, I. Pastan, and M. M. Gottesman. Photosensitized labeling of a functional multidrug transporter in living drug-resistant tumor cells. *J. Biol. Chem.* **265**:3975–3980 (1990).
3. C. F. Higgins and M. M. Gottesman. Is the multidrug transporter a flippase? *Trends Biochem. Sci.* **17**:18–21 (1992).

4. L. Homolya, Z. Hollo, U. A. Germann, I. Pastan, M. M. Gottesman, and B. Sarkadi. Fluorescent cellular indicators are extruded by the multidrug resistance protein. *J. Biol. Chem.* **268**:21493–21496 (1993).
5. C. F. Higgins and K. J. Linton. The ATP switch model for ABC transporters. *Nat. Struct. Mol. Biol.* **11**:918–926 (2004).
6. W. D. Stein, C. Cardarelli, I. Pastan, and M. M. Gottesman. Kinetic evidence suggesting that the multidrug transporter differentially handles influx and efflux of its substrates. *Mol. Pharmacol.* **45**:763–772 (1994).
7. F. J. Sharom. The P-glycoprotein efflux pump: how does it transport drugs? *J. Membr. Biol.* **160**:161–175 (1997).
8. R. Kikuchi, H. Kusuhara, D. Sugiyama, and Y. Sugiyama. Contribution of organic anion transporter 3 (Slc22a8) to the elimination of *p*-aminohippuric acid and benzylpenicillin across the blood–brain barrier. *J. Pharmacol. Exp. Ther.* **306**:51–58 (2003).
9. S. Mori, H. Takanaga, S. Ohtsuki, T. Deguchi, Y. S. Kang, K. Hosoya, and T. Terasaki. Rat organic anion transporter 3 (rOAT3) is responsible for brain-to-blood efflux of homovanillic acid at the abluminal membrane of brain capillary endothelial cells. *J. Cereb. Blood Flow Metab.* **23**:432–440 (2003).
10. W. D. Stein. Kinetics of the multidrug transporter (P-glycoprotein) and its reversal. *Physiol. Rev.* **77**:545–590 (1997).
11. P. L. Golden and G. M. Pollack. Rationale for influx enhancement *versus* efflux blockade to increase drug exposure to the brain. *Biopharm. Drug. Dispos.* **19**:263–272 (1998).
12. S. H. Jang, M. G. Wientjes, and J. L. Au. Interdependent effect of P-glycoprotein-mediated drug efflux and intracellular drug binding on intracellular paclitaxel pharmacokinetics: application of computational modeling. *J. Pharmacol. Exp. Ther.* **304**: 773–780 (2003).
13. J. R. Pappenheimer and B. P. Setchell. Cerebral glucose transport and oxygen consumption in sheep and rabbits. *J. Physiol.* **233**: 529–551 (2003).
14. A. Gjedde and O. Christensen. Estimates of Michaelis-Menten constants for the two membranes of the brain endothelium. *J. Cereb. Blood Flow Metab.* **4**:241–249 (1984).
15. V. J. Cunningham, R. J. Hargreaves, D. Pelling, and S. R. Moorhouse. Regional blood–brain glucose transfer in the rat: a novel double-membrane kinetic analysis. *J. Cereb. Blood Flow Metab.* **6**:305–314 (1986).
16. G. A. Oyler, R. B. Duckrow, and R. A. Hawkins. Computer simulation of the blood–brain barrier: a model including two membranes, blood flow, facilitated and non-facilitated diffusion. *J. Neurosci. Methods* **44**:179–196 (1992).
17. H. Ashida, T. Oonishi, and N. Uyesaka. Kinetic analysis of the mechanism of action of the multidrug transporter. *J. Theor. Biol.* **195**:219–232 (1998).
18. R. N. Upton. Theoretical aspects of P-glycoprotein mediated drug efflux on the distribution volume of anaesthetic-related drugs in the brain. *Anaesth. Intensive Care* **30**:183–191 (2002).
19. H. Sun, P. M. Bungay, and W. F. Elmquist. Effect of capillary efflux transport inhibition on the determination of probe recovery during *in vivo* microdialysis in the brain. *J. Pharmacol. Exp. Ther.* **297**:991–1000 (2001).
20. I. Szentistvanyi, C. S. Patlak, R. A. Ellis, and H. F. Cserr. Drainage of interstitial fluid from different regions of rat brain. *Am. J. Physiol.* **246**:F835–F844 (1984).
21. M. Hammarlund-Udenaes. The use of microdialysis in CNS drug delivery studies. Pharmacokinetic perspectives and results with analgesics and antiepileptics. *Adv. Drug Deliv. Rev.* **45**:283–294 (2000).
22. E. C. Langede and M. Danhof. Considerations in the use of cerebrospinal fluid pharmacokinetics to predict brain target concentrations in the clinical setting: implications of the barriers between blood and brain. *Clin. Pharmacokinet.* **41**:691–703 (2002).
23. W. M. Pardridge. Log(BB), PS products and *in silico* models of drug brain penetration. *Drug Discov. Today* **9**:392–393 (2004).
24. MathWorks. *MATLAB The Language of Technical Computing; Using MATLAB*, MathWorks, Natick, MA, 2002.
25. B. Davies and T. Morris. Physiological parameters in laboratory animals and humans. *Pharm. Res.* **10**:1093–1095 (1993).
26. W. M. Pardridge, D. Triguero, J. Yang, and P. A. Cancilla. Comparison of *in vitro* and *in vivo* models of drug transcytosis through the blood–brain barrier. *J. Pharmacol. Exp. Ther.* **253**:884–891 (1990).
27. C. Nicholson and J. M. Phillips. Ion diffusion modified by tortuosity and volume fraction in the extracellular microenvironment of the rat cerebellum. *J. Physiol.* **321**:225–257 (1981).
28. R. Xie, M. R. Bouw, and M. Hammarlund-Udenaes. Modelling of the blood–brain barrier transport of morphine-3-glucuronide studied using microdialysis in the rat: involvement of probenecid-sensitive transport. *Br. J. Pharmacol.* **131**:1784–1792 (2000).
29. M. R. Bouw, R. Xie, K. Tunblad, and M. Hammarlund-Udenaes. Blood–brain barrier transport and brain distribution of morphine-6-glucuronide in relation to the antinociceptive effect in rats—pharmacokinetic/pharmacodynamic modelling. *Br. J. Pharmacol.* **134**:1796–1804 (2001).
30. K. Tunblad, M. Hammarlund-Udenaes, and E. N. Jonsson. Influence of probenecid on the delivery of morphine-6-glucuronide to the brain. *Eur. J. Pharm. Sci.* **24**:49–57 (2005).
31. K. Tunblad, E. N. Jonsson, and M. Hammarlund-Udenaes. Morphine blood–brain barrier transport is influenced by probenecid co-administration. *Pharm. Res.* **20**:618–623 (2003).
32. Y. Wang and D. F. Welty. The simultaneous estimation of the influx and efflux blood–brain barrier permeabilities of gabapentin using a microdialysis–pharmacokinetic approach. *Pharm. Res.* **13**:398–403 (1996).
33. S. Mori, S. Ohtsuki, H. Takanaga, T. Kikkawa, Y. S. Kang, and T. Terasaki. Organic anion transporter 3 is involved in the brain-to-blood efflux transport of thiopurine nucleobase analogs. *J. Neurochem.* **90**:931–941 (2004).
34. C. Dagenais, C. L. Graff, and G. M. Pollack. Variable modulation of opioid brain uptake by P-glycoprotein in mice. *Biochem. Pharmacol.* **67**:269–276 (2004).
35. H. Takanaga, H. Murakami, N. Koyabu, H. Matsuo, M. Naito, T. Tsuruo, and Y. Sawada. Efflux transport of tolbutamide across the blood–brain barrier. *J. Pharm. Pharmacol.* **50**: 1027–1033 (1998).
36. S. Cisternino, C. Rousselle, M. Debray, and J. M. Scherrmann. *In situ* transport of vinblastine and selected P-glycoprotein substrates: implications for drug–drug interactions at the mouse blood–brain barrier. *Pharm. Res.* **21**:1382–1389 (2004).
37. M. Dogruel, J. E. Gibbs, and S. A. Thomas. Hydroxyurea transport across the blood–brain and blood–cerebrospinal fluid barriers of the guinea-pig. *J. Neurochem.* **87**:76–84 (2003).